Desalination and Water Treatment
www.deswater.com

doi: 10.1080/19443994.2015.1084533

57 (2016) 16679–16702
August

Taylor & Francis
Taylor & Francis Group

PV and CSP solar technologies & desalination: economic analysis

M.A. Darwish, H.K. Abdulrahim*, A.S. Hassan, A.A. Mabrouk

Qatar Environment and Energy Research Institute, HBKU, Qatar Foundation, P.O. Box 5825, Doha, Qatar, Tel. +974 44545880; email: madarwish@qf.org.qa (M.A. Darwish), Tel. +974 44545884; email: habdelrehem@qf.org.qa (H.K. Abdulrahim), Tel. +974 44545887; email: ahassan@qf.org.qa (A.S. Hassan), Tel. +974 44547453; email: aaboukhlewa@qf.org.qa (A.A. Mabrouk)

Received 12 February 2015; Accepted 11 August 2015

ABSTRACT

This paper presents an overview of using solar energy in running desalination systems, called solar desalination. Solar energy can be converted directly to electric energy, which can operate electrically driven desalting systems such as reverse osmosis (RO), electrodialysis (ED), and mechanical vapor compression systems. Solar energy can also be converted to the thermal energy that can operate the mainly used thermally operated desalination system such as multistage flash (MSF), conventional multieffect (ME), and multieffect thermal vapor compression (ME-TVC), and emerging membrane distillation and humidification–dehumidification desalination systems. The thermal energy converted from solar energy can also be used to produce high-pressure steam running power plant producing electric power to operate mechanically driven desalting systems, and/or extracted steam at relatively low pressure to operate thermally driven desalting system. The main obstacle that hinders the use of solar desalination is the initial investment cost. This paper discusses the use of the solar desalination and calculates the investment cost to install solar desalination plants. These include photovoltaic (PV)-driven RO system, and thermally driven MSF and ME plants by steam directly generated by solar collectors, or by steam extracted from solar steam power plants operated by the concentrated solar collectors. The results revealed that PV-RO desalting system has the highest specific capital cost, among the considered systems, because the expensive storage of the electric energy in batteries, and the fact solar energy supply lasts about one third of the day. It showed also that using the thermally generated energy from concentrated solar collectors operating power plant is much cheaper than using this thermal energy when directly operating the desalination system.

Keywords: CSP solar energy; Photovoltaic; Reverse osmosis; MED; Water cost

1. Introduction

Water scarcity is a real problem in the Gulf Cooperation Countries (GCC) block, including Saudi Arabia (SA), United Arab Emirates (UAE), Kuwait, Qatar, Bahrain, and Oman. Water demands in GCC are far beyond renewable fresh water resources. The ratio of water consumed per capita to renewable fresh water resources per capita is 39 in UAE, 11 in SA, 12 in Qatar, 63 in Kuwait, 4.4 in Bahrain, and 1 in Oman [1]. Groundwater (GW) is over-extracted to satisfy parts of demands, and thus the GW is depleted at much higher rate than replenishing.

*Corresponding author.

Desalted seawater (DW) plays a major share in satisfying fresh water demands, especially municipal water (e.g. 99% in Qatar, and 96% in Kuwait). The share of DW to total water withdrawal is 79% in Bahrain, 75% in Qatar, 69% in Kuwait, 67% in UAE, 44% in Oman, and 14% in SA. It is only in the GCC where DW has that high share of total water withdrawal. The global percentage share of desalination capacity between the major DW producing countries is shown in Fig. 1 [2].

Demands for DW in GCC are always on the rise due to increases in population and standard of living. As example, Qatar consumed DW increase from 178 Mm^3/y in 2004 to 465 Mm^3/y in 2013, more than 2.6 times increase in 9 years. More desalting plants are continuously needed and added. DW production is expensive and consumes too much fossil fuel, especially in the GCC, when compared with groundwater (GW) extraction, or treating wastewater. Moreover, DW is produced in GCC by the highly energy consumed thermally operated desalting plants, compared with the most used, worldwide, seawater reverse osmosis (SWRO) desalting plants. The DW represents good share of municipal water in GCC, e.g. 99% in Qatar, 96% in Kuwait, and 66% in SA, and thus it represents good share of total water withdrawal. The consumed fuel cost represents good share of the total DW production cost. All GCC, except Qatar, are struggling to secure natural gas (NG) needed to run their cogeneration power desalting plants (CPDP), which produce both electric power and DW.

Dependence of DW on burning fossil fuel emits greenhouse gasses, mainly CO_2; and negatively affects marine environment by discharging brine of about 50% higher salinity and higher temperature (about 10˚C) than the intake seawater. There are claims that the Gulf water salinity and temperature have increased about 2 percent over the last 20 years [1].

Using solar energy to produce DW, called solar desalination, provides free clean and secure energy source, minimizes dependence on fossil fuels, reduces greenhouse gases emission, and provides sustainable source of potable water. The high solar intensity in GCC encourages the idea of utilizing solar energy to solve the water scarcity problem. It is unfortunate that application of solar desalination still restricted to small-scale systems designed for remote areas because of its high cost. Solar desalination involves combining solar radiation conversion to heat or electricity with DPs.

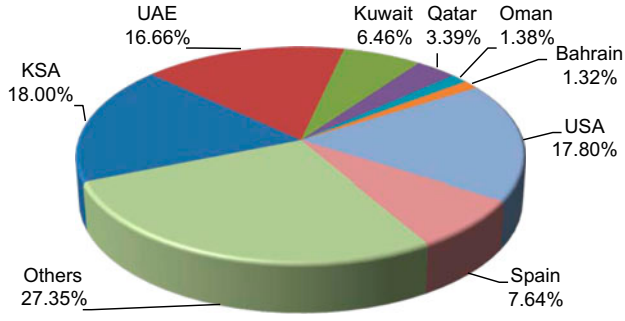

Fig. 1. The share of desalination capacity worldwide [2].

2. Desalination systems

Desalting methods can be classified as distillation and membranes processes. In distillation, vapor is generated from seawater and then condensed as pure water. Vapor is generated from SW either by boiling or by flashing. The most commonly used thermally driven distillation methods are multistage flash (MSF), multieffect boiling or distillation (MED), thermal vapor compression (TVC), and combination of MED–TVC. Another distillation process is the mechanical vapor compression (MVC) desalting system. It is mechanically driven by compressor operated by a motor, diesel engine, or gas or steam turbine. The thermally operated desalting systems need extra pumping energy to move their streams. The commercial desalination systems are summarized in the following sections.

2.1. MSF desalination system

The MSF is the most used desalting system in GCC, and is operated with top brine temperature (TBT) in the range of 110˚C, and its heating steam supply (S) to the brine heater has saturation temperature (S.T.) in the range of 120˚C. In flashing, seawater (or brine) is heated to a temperature, say T_o, and exposed to a pressure having S.T. = T_v less than T_o, i.e. $T_v < T_o$. Then, the seawater temperature has drops to T_v to reach equilibrium by flashing (evaporation). This vapor is then condensed giving its thermal energy to the feed water for energy recovery. It is usually rated by the gain ratio (GR) defined by the distillate output (D) to S, i.e. GR = D/S, and by specific consumed heat Q divided by D, or (Q/D). The MSF units operating in GCC has GR ranging from 6 to 10, and Q/D ranging from 250 to 300 MJ/m^3. Also pumping energy is consumed by the MSF to move its streams with typical specific pumping work (W_p) divided by D, or W_p/D in the range of 3.5–4.5 kW h/m^3. The specific consumed fuel energy (Q_f/D), counting for both thermal and pumping have a typical value of 340 MJ/m^3 when the

steam is supplied to MSF directly from a boiler, and 200 MJ/m^3 when extracted from steam turbine. More details on the MSF desalting system are given in Ref. [3].

2.2. MED desalination system

The MED is more energy efficient than the MSF system. It is rated also by GR and Q/D as the MSF, and has typical Q/D = 200–300 MJ/m^3. However, most operating MED have TBT in the range of 65°C, and heating steam supply to the first effect can have S.T. in the range of 70°C. This steam has low availability (energy) than that supplied to the MSF. This allows the heating steam when extracted from steam turbine to expand more and give more work before being extracted to the MED units. Therefore, the equivalent work supplied to the MED is less than that supplied to the MSF because its S.T. is lower than that used in the MSF. Moreover, the MED consumes less pumping energy (about half that used in the MSF system). The specific consumed fuel energy (Q_f/D) counting for both thermal and pumping has a typical value of 320 MJ/m^3 when the steam is supplied to MED directly from boiler, and 140 MJ/m^3 when extracted from steam turbine. More details on the MED desalting system are given in Ref. [4].

2.3. TVC desalination system

In TVC distillation process, part of the generated steam in the last effect is compressed to become a heating steam by a steam ejector utilizing a high-pressure motive steam. The motive steam supply to the steam ejector is expanding in a nozzle to a low pressure (lower than the vapor in the last effect) to extract part of the generated vapor. The mixture of the expanded steam and extracted vapor passes through a diffuser to increase its pressure on the expense of its velocity, and utilize it as a heating steam in the first effect at a typical S.T. of 70°C. This system is also rated by the gain ratio GR = D/S, (S here is the motive steam in this case), and specific consumed heat Q/D, (Q is the heat supplied with the motive steam). The motive steam in the TVC system does not directly heat the seawater, but is used to raise the pressure of the extracted vapor to become a heating steam. Therefore, it can be at much higher S.T. than the TBT, and thus has high availability. The main obstacle of this system is the limited capacity of the steam ejectors. Therefore, high capacity units are arranged with two TVC units operating in parallel, and conventional MED is operating in series with them. The compressed vapor has higher pressure and thus lower specific volume than that supplied to the end condenser. Typical values of a large MED–TVC are: $P_{\text{motive steam}}$ (3–20) bar, GR (8–16), Q/D (150–300) MJ/m^3, W_{pumping}/D = 2 kW h/m^3, and Q_{fuel}/D = 200 MJ/m^3 in CPDP, and 360 MJ/m^3 for boiler operated system. More details on the TVC desalting system are given in Ref. [4].

2.4. RO desalination system

The membrane desalting systems include reverse osmosis (RO), where seawater is pressurized against a semipermeable membrane that allows almost pure water to permeate, and not salt. It is mechanically driven by pumping energy. The main problem of the SWRO is the membrane's fouling that required extensive pretreatment to avoid or decrease that fouling. The feed water pressure (P_f) to the membranes is in the range of 60–80 bar (depending on the feed water salinity, and membranes characteristics). The brine leaving the membranes is at about 2 or 3 bar only less than P_f. The energy of this brine can be recovered by energy recovery device (ERD), (e.g. reversed centrifugal pump working as a turbine, Pelton wheel, and pressure exchanger). The specific consumed energy is in the range of 4–6 kW h/m^3 depending on the feed water salinity and the type of ERD. The share of RO membrane process is rapidly increasing with the time compared to distillation processes as it consumes much less energy, and thus less cost, see Fig. 2.

2.5. Other desalination system

Other membrane desalination methods include electro-dialysis (ED), and membrane distillation (MD). Other distillation systems include humidification–dehumidification (HDH). In ED desalination process, direct electric current is applied across flowing saline water to drive ions across anions and cations exchange permeable membrane, and then dilutes the coming saline water. The required energy for the ED depends on the initial salinity of the saline water. It is mainly applied to desalt brackish water, although its use for high salinity water is now promising. MD is a hybrid thermal membrane process that can use low-grade waste heat to generate a vapor pressure difference across a hydrophobic membrane to produce a high quality distillate from concentrated brines. The HDH is a thermal water desalination method. It is based on evaporation of seawater or brackish water and consecutive condensation of the generated humid air, mostly at the ambient pressure. Both MD and HDH can be operated by relatively low temperature heating

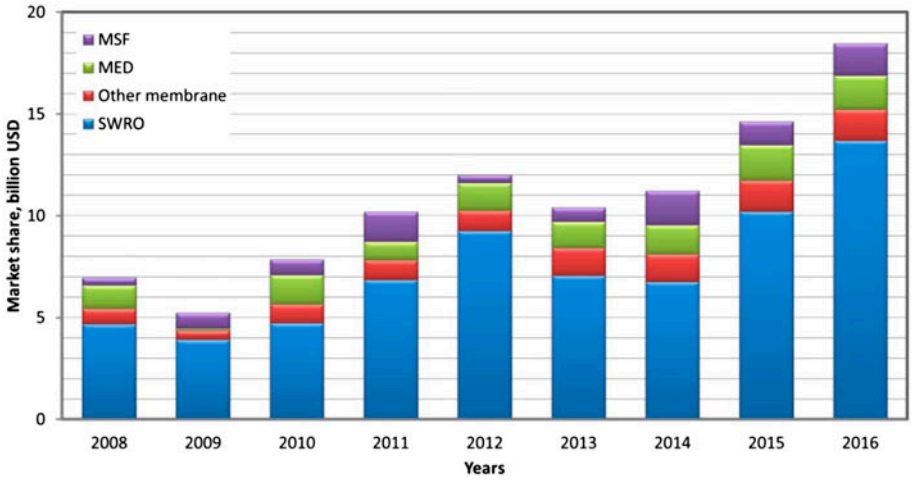

Fig. 2. The trend of increasing use of RO compared to distillation processes [2].

sources that can be easily provided by flat or evacuated solar collectors.

3. Solar desalination technologies

There are many variants for solar desalination, as summarized in Fig. 3.

3.1. Direct solar electricity–desalination system

Photovoltaic cells can be used to operate mechanically (or electrically) driven desalting systems such as SWRO, MVC, or ED. Example of a prototype commercial system of RO plant is provided with an energy recovery system in the water stream built in Doha, Qatar. It produces 5.7 m^3/d (1,500 gpd) fresh water powered by a photovoltaic array of 11.2 kW-peak [5]. More discussion of this system is given later.

3.2. Direct solar thermal operated desalination system

Solar stills: a solar still is a shallow basin holding seawater enclosed by a canopy, transparent to solar radiation. The incident short wave radiation is transmitted and absorbed as heat. To ensure maximum absorption of solar radiation, the basin surface is blackened. A simple solar still yields very little water: 5 L/d/m^2 is a typical best, meaning that 3-m^3/d would require an area of 600 m^2. For this reason, solar still is not to be considered here. This can be compared with PV-SWRO that requires only 40 m^2 of PV to produce the same capacity using non-concentrating collector intercepting and absorbing solar radiation and convert it to heat flowing fluid that operate the desalting plant. Examples are the use evacuating tube collectors operating 120 m^3/d MED desalting unit in Abu Dhabi, and 40 m^3/d ME desalting unit in La Desired Island, French Caribbean [5].

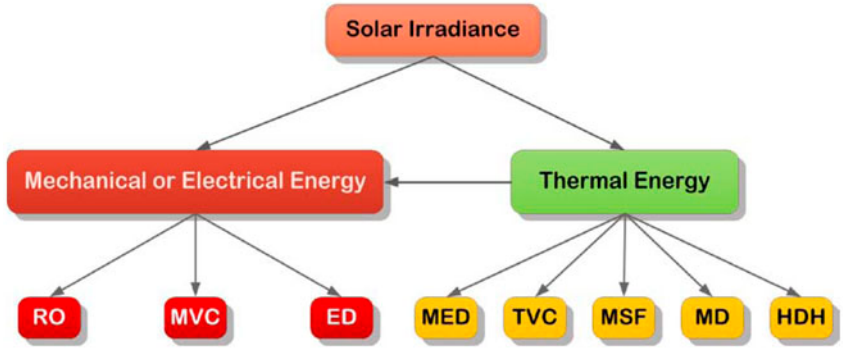

Fig. 3. Solar desalination variants.

(1) Using non-concentrating collector intercepting and absorbing solar radiation and convert it to heat flowing fluid that operates the desalting plant. Examples are the use of evacuating tube collectors operating 120 m^3/d MED desalting unit in Abu Dhabi, and 40 m^3/d ME desalting unit in La Desired Island, French Caribbean [5].
(2) Using concentrating solar power (CSP) collectors that concentrate solar rays on an absorber to produce steam directly as in linear Fresnel collectors (LFC), or to heat oil that generates steam in heat exchanger as in parabolic trough collector (PTC). The generated steam can directly drives thermal desalting system such as MSF, Fig. 4, or multieffect distillation (MED) desalting systems, Fig. 5. An example is a 100 m^3/d MSF desalting unit in Kuwait, and is called stand-alone desalting arrangement [3].

3.3. Indirect solar thermal desalting system

(1) Using the steam generated by the concentrated solar power (CSP) collectors to drive solar power plant (SPP) that produces electric power operating mechanically driven desalting systems such as SWRO or MVC desalting systems, Figs. 6 and 7.
(2) Using steam extracted from steam turbine of a SPP to drive MSF or MED plant, besides utilizing the electric power to operate SWRO or MVC desalting system. Fig. 8 shows SPP driving MED and SWRO.
(3) Using integrated solar gas/steam combined cycle (ISCC) to produce EP and extracted steam to operate desalting systems, Fig. 9.

4. RO using photovoltaic (PV) cells

Many PV-operated SWRO desalting systems were built, but for small capacities, mainly in the range of 1–5 m^3/d. Desalination by RO is the leading desalting system, worldwide, as it consumes much lower energy compared to distillation methods. Driving the RO desalting system with PV proves to be technically and economically feasible for remote areas with access to sea or brackish water. The PV technology is rapidly growing with declining prices, Figs. 10 and 11. Costs of solar modules account for 40–50% of total PV system cost.

Figs. 10 and 11 present the average retail prices in Europe and the USA based on a monthly online survey.

They encompass a wide range of module prices, varying according to the module technology (with thin film modules generally cheaper than c-Si), the module model and manufacturer, its quality, as well as the country in which the product is purchased. For example, in March 2012 average retail module prices were, respectively, 2.29\$/W_p in USA and 2.17€/W_p in Europe, but the lowest retail price for a crystalline silicon solar module was 1.1\$/W_p (0.81€/W_p) and the lowest thin film module price was 0.84\$/W_p (0.62€/W_p) [7].

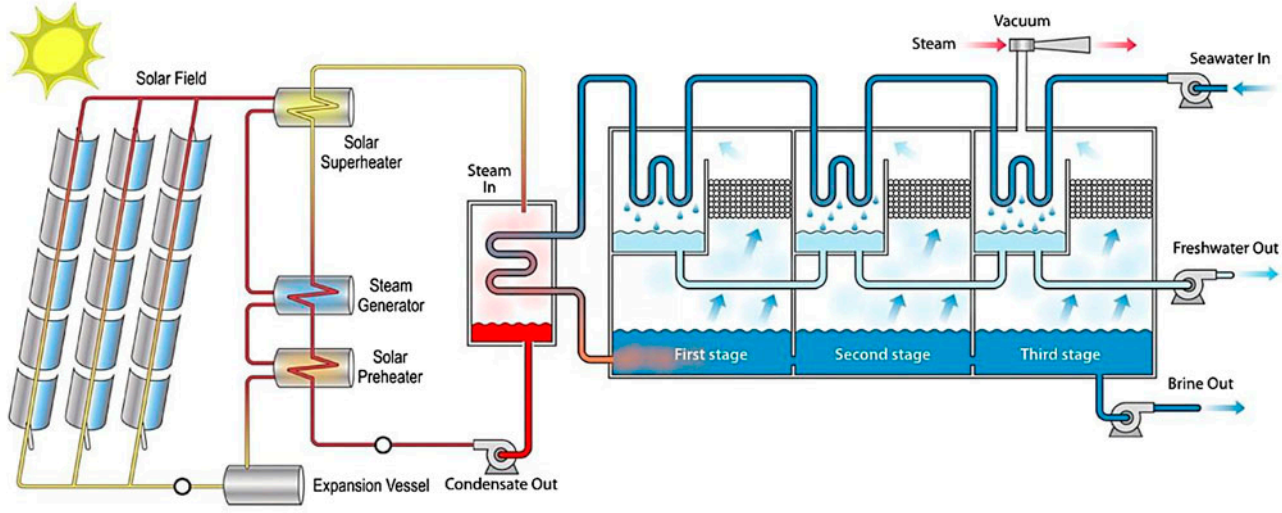

Fig. 4. Solar PTC operating MSF unit.

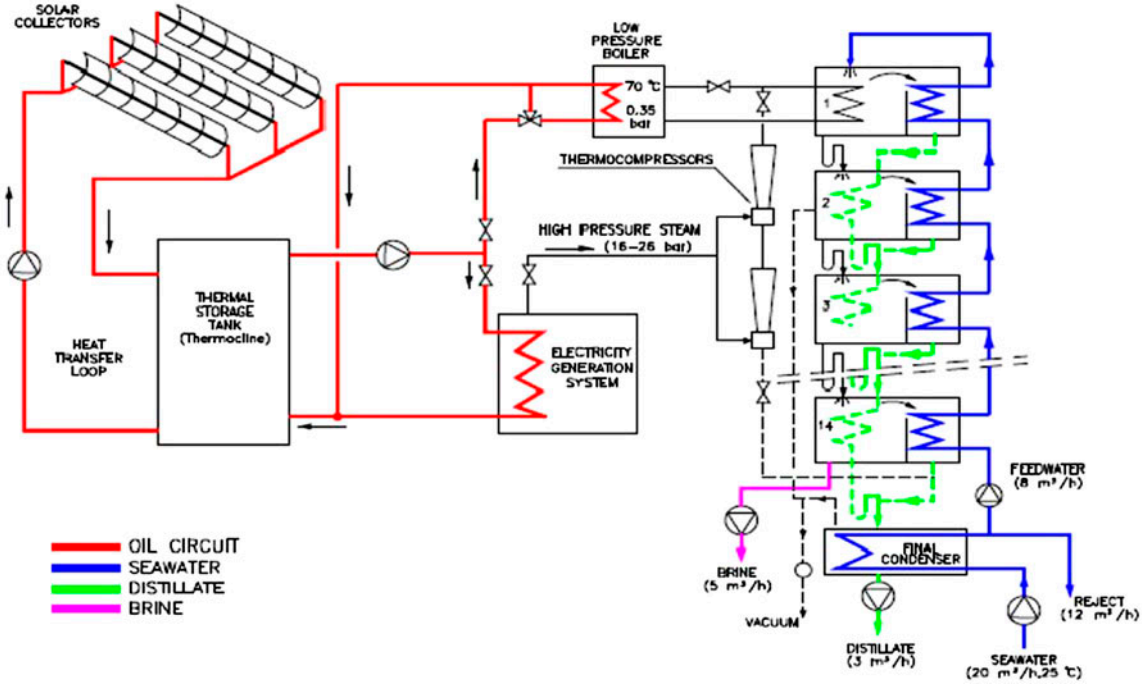

Fig. 5. Solar PTC operating MED unit.

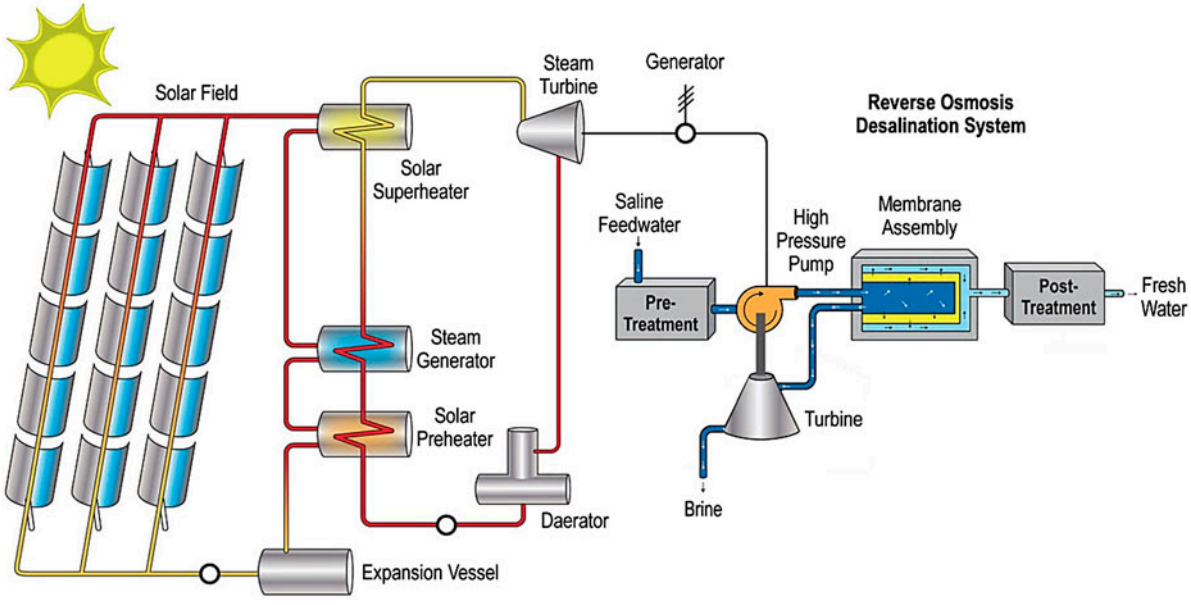

Fig. 6. SPP with its EP output operating SWRO desalting system.

A photovoltaic or "solar cell" is a semiconductor device that directly converts sunlight to direct current (DC) electricity. The materials most commonly used in PV manufacturing are mono-crystalline silicon (Si), multicrystalline Si, and compounds of cadmium sulfide (CdS), cuprous sulfide (Cu_2S), and gallium arsenide (GaAs). These cells are packed into modules, which produce a specific DC voltage and current when illuminated.

A silicon solar cell produces, under intense sun, more than 30 mA/cm^2. So, a commercial cell of 12.5 × 12.5 cm^2 gives about (12.5 × 12.5 × 30/1,000≅)

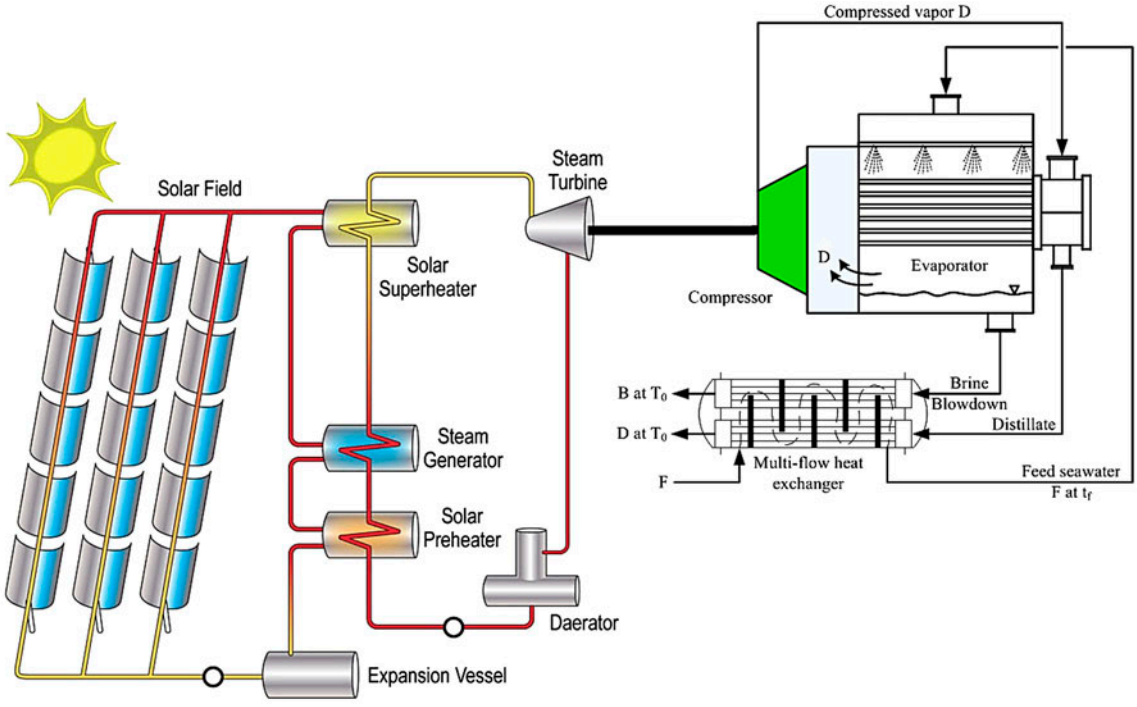

Fig. 7. SPP with its EP output operating MVC desalting system.

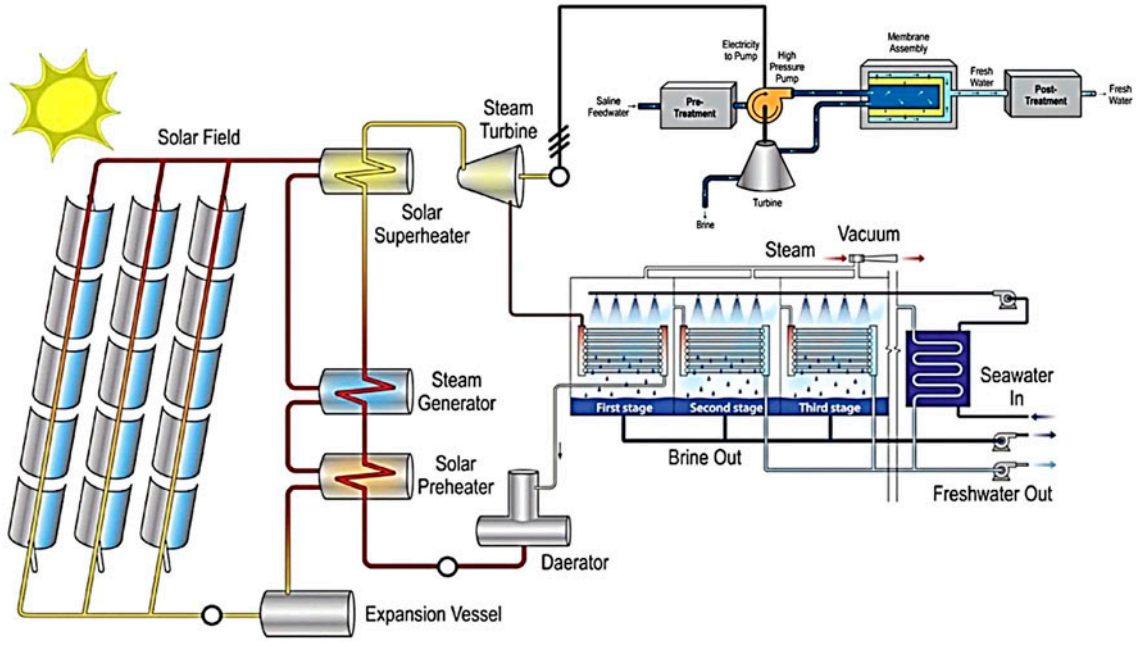

Fig. 8. SPP using PTC with EP output operating RO plant, and steam discharged from steam turbine operating MSF unit.

5 A of DC, at a voltage lower than 0.5 V gives less than 2.5 W of electric power. This is too low and as a result, several cells are to be associated to add generation capabilities. About 30–36 PV solar cells are connected to build a module, several modules are connected to form a panel, and several panels form an

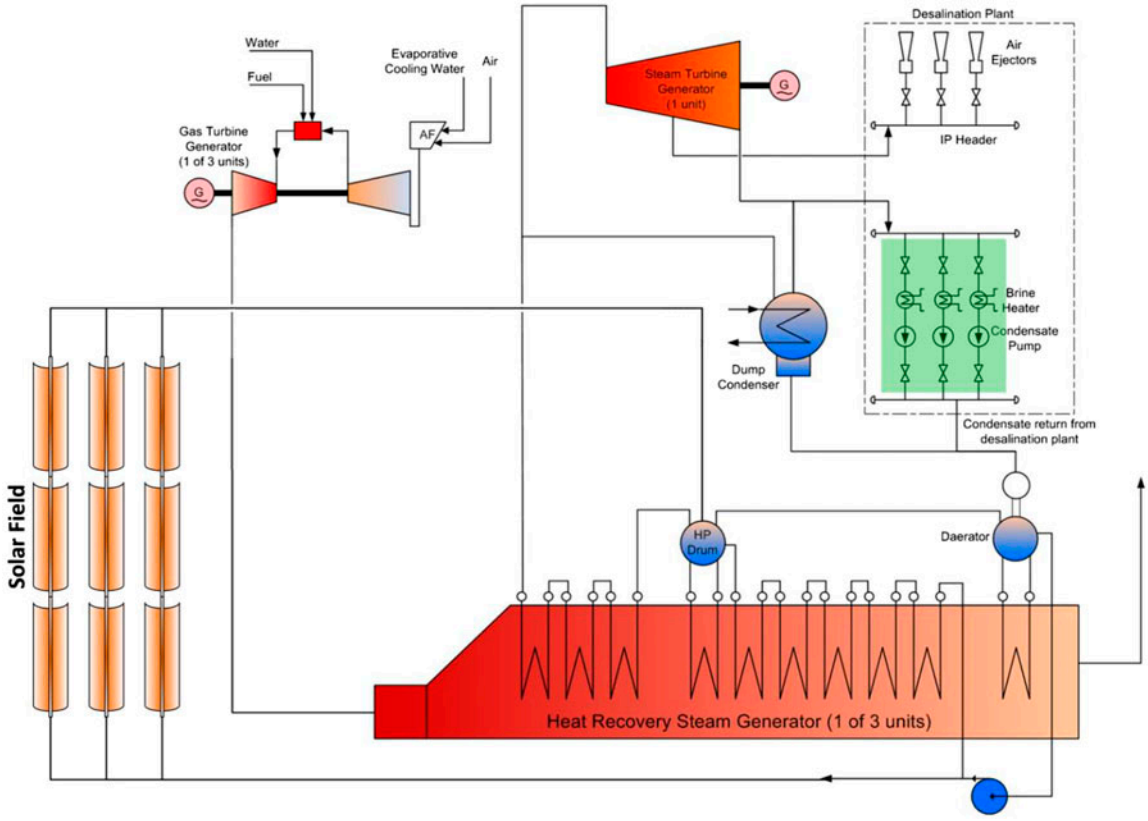

Fig. 9. Integrated solar combined cycle.

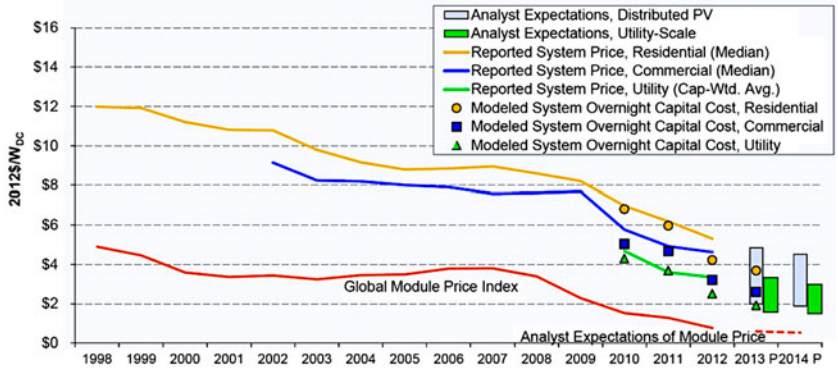

Fig. 10. Reported, bottom-up, and analyst-projected average U.S. PV system prices over time [6].

array. For a module of 36 (or 72) cells conned in series, and each cell produces about 0.5 V in sunlight, it gives 18 V (or 36), Fig. 12(a), and enables the panel to charge 12 V (or 24 V) batteries. The 36 panel with 18 V will charge the batteries better than the 30-cell panel, but it needs control to avoid over-charging. The main electrical and mechanical characteristics of a typical mono-crystalline silicon module are: maximum power rating = 85 W, open-circuit voltage (V_{OC}) = 22 V, short-circuit current (I_{SC}) = 5 A, voltage at maximum power = 18 V, current at maximum power = 4.7 A, length = 1,188 mm, width = 530 mm, depth = 44 mm, and weight = 7.5 kg. The power rating of PV modules is typically given in watts peak (W_p)

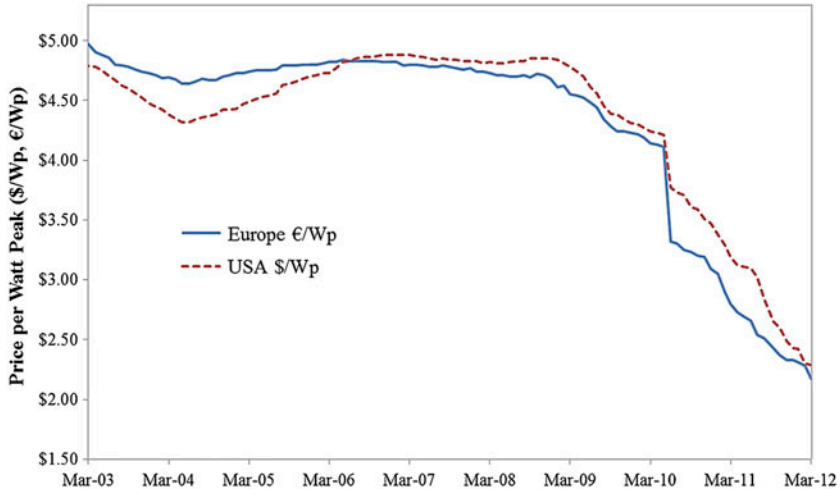

Fig. 11. PV module retail price index (2003–2012, €2,012 and $2,012) [6].

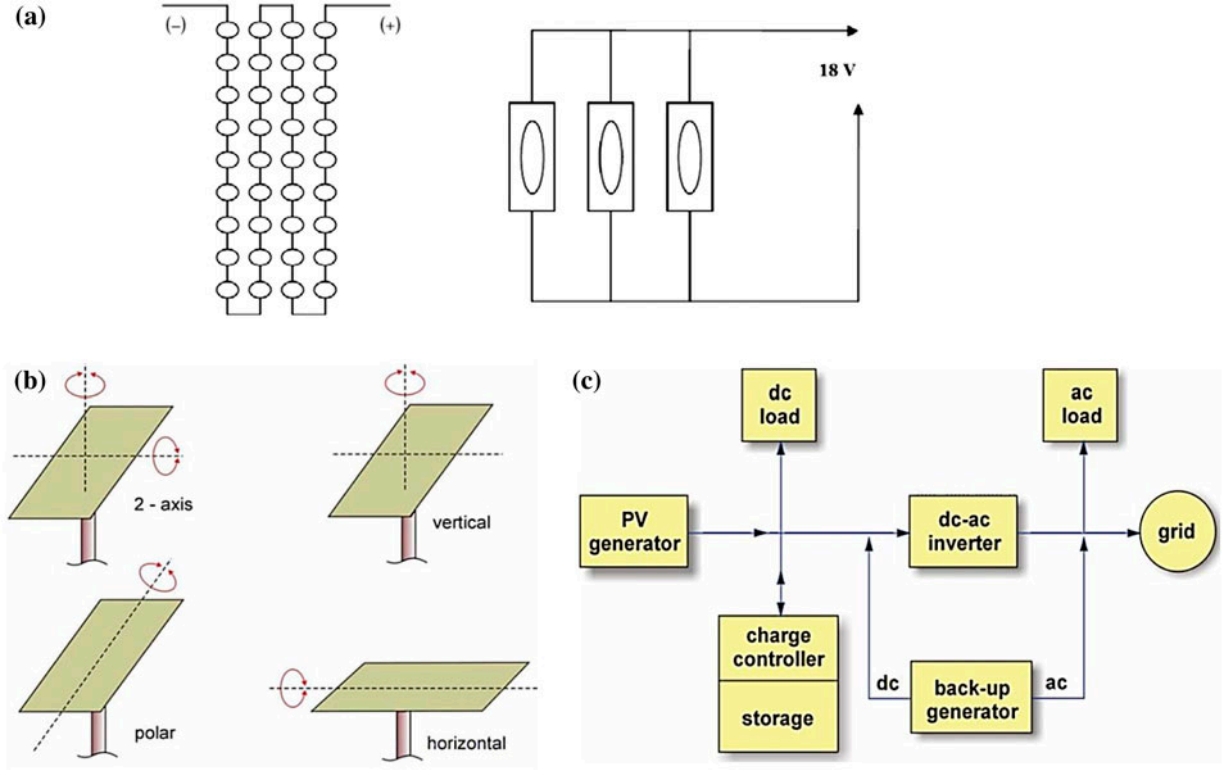

Fig. 12. (a) Typical arrangements of commercial Si solar cells; module of 36 cells array, and 3 modules forming panel, (b) tracking modes[9] and (c) general photovoltaic system [8].

and refers to the maximum power output under standard test conditions. The output voltage of PV modules typically matches the charging voltage of a 12 V battery, allowing for voltage losses in cables and control equipment.

The array is arranged for practical devices, which require a particular voltage or current for their operation. The solar panels are the heart of a complete PV solar system. Other parts include mounting structures carrying the modules in direction of the sun. A PV

array could be mounted on a sun tracking system, Fig. 12(b), if the additional cost is justified. Storage of energy is required to operate the load during non-illuminating time using batteries as storage system. The PV power outputs depend on sunlight intensity and temperature, and thus vary with time. Therefore, the DC output delivered to batteries, grid, and/or load is to be controlled for a smooth operation of the PV system. The control components are called charge regulators; see Fig. 12(c).

The power input to a PV system is the solar irradiance, which is luminous power per unit area and conveniently expressed in kW/m^2. The sum of the direct and diffuse components is called the global irradiance.

If irradiance is integrated over a period of time (usually, an hour, a day or a year), the irradiation, which is the energy received per unit surface in that period of time, in kW h/m^2 is obtained. PV modules can receive more energy per unit area if they are tilted an angle equal to the latitude. As example, the daily global irradiance and environmental temperature (affecting the PV current output) are given in Figs. 13 and 14 in Al-Khor, Qatar. Fig. 13 shows the annual daily average is 5.122 kW h/m^2 with a maximum of 6.463 kW h/m^2 in June and 3.498 kW h/m^2 in December.

PV electrical parameters are determined at standard test conditions, i.e. 1,000 W/m^2 solar irradiance, 25˚C cell temperature and air mass (AM) 1.5 solar radiations. Rated specifications from typical PV module are determined from the maximum power point (MPP) of the illuminated *I–V* characteristics.

The resulted current and power are related to the solar intensity, Figs. 15–17 and their variation with temperature are shown in Fig. 18. In order to guarantee performance specifications of modules, modules are sealed for protection against corrosion, moisture, pollution, and weathering.

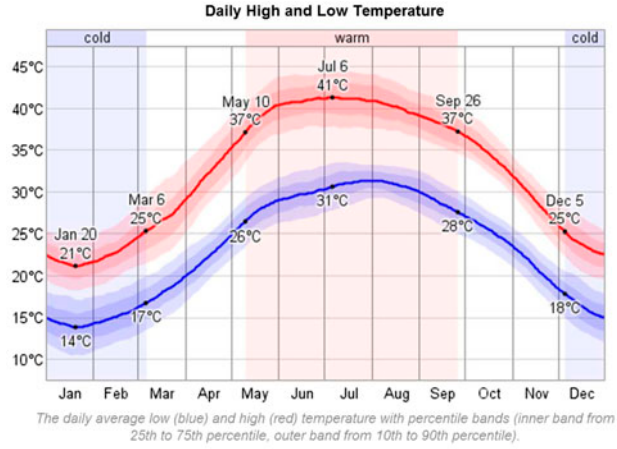

Fig. 14. Ambient daily high and low temperature by month in Al-Khor, average weather for Doha, Qatar [10].

Individual modules may have cells connected in series and parallel combinations. In series connection, the voltage is the sum of those of the individual devices; in a parallel connection, the currents add up, Fig. 19. In a commercial module, the cells are usually connected in series.

Variation of both solar insolation and temperature through the day causes the *I–V* curve to vary, and thus the MPP is not stationary. To maintain operation close to the MPP is known as maximum power point tracking (MPPT) and is critical to the efficient operation of a PV-RO system.

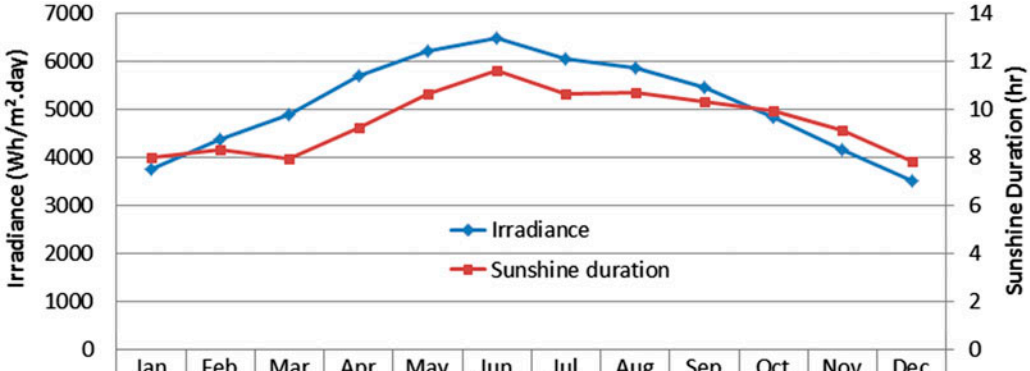

	Jan	Feb	Mar	Apr	May	Jun	Jul	Aug	Sep	Oct	Nov	Dec
Irradiance	3749	4366	4893	5699	6204	6463	6051	5847	5458	4817	4149	3498
Sunshine duration	8	8.3	7.9	9.2	10.6	11.6	10.6	10.7	10.3	9.9	9.1	7.8

Fig. 13. Solar radiation levels by month in Al-Khor, Qatar [9].

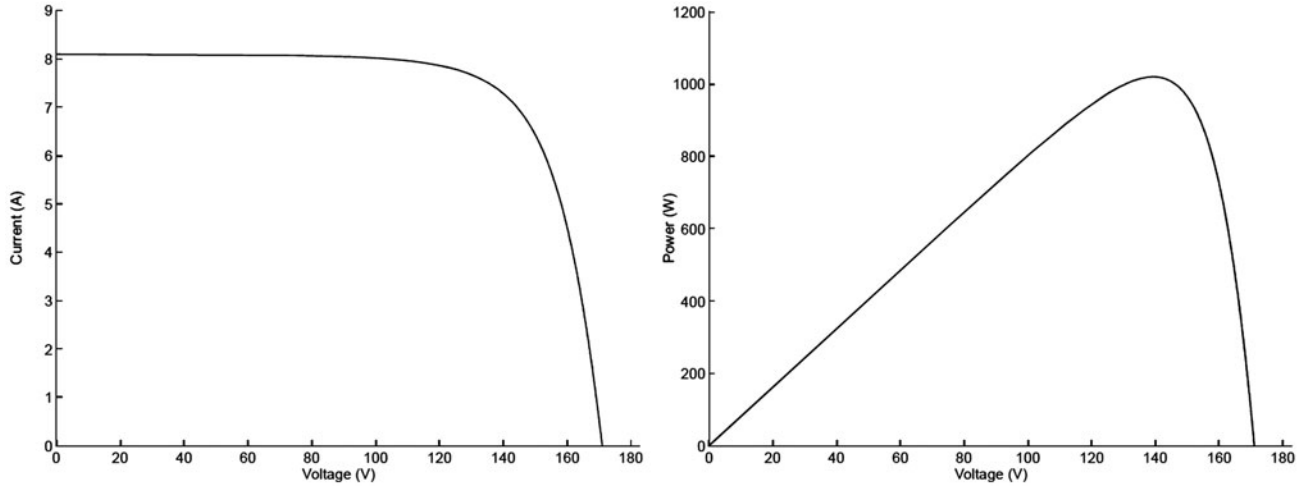

Fig. 15. Typical *I–V* and *P–V* curves for a polycrystalline-silicon PV array [11].

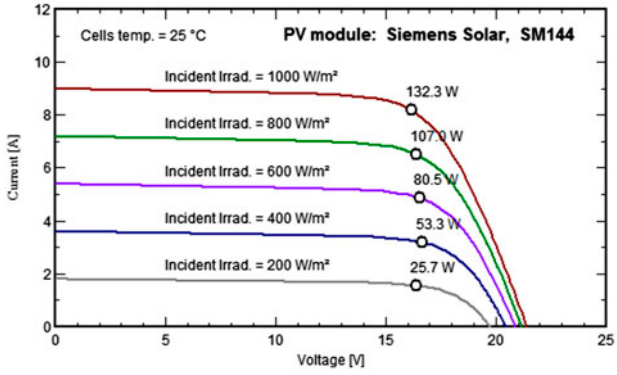

Fig. 16. The effect of solar irradiance on the PV electric power output for a typical module [12].

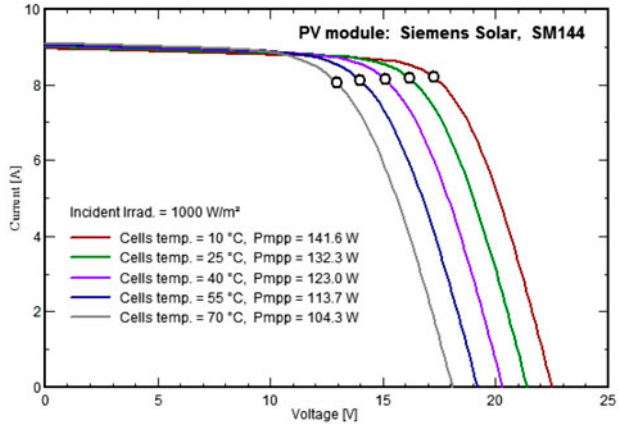

Fig. 18. The effect of ambient temperature on *I–V* PV output, for a typical module [12].

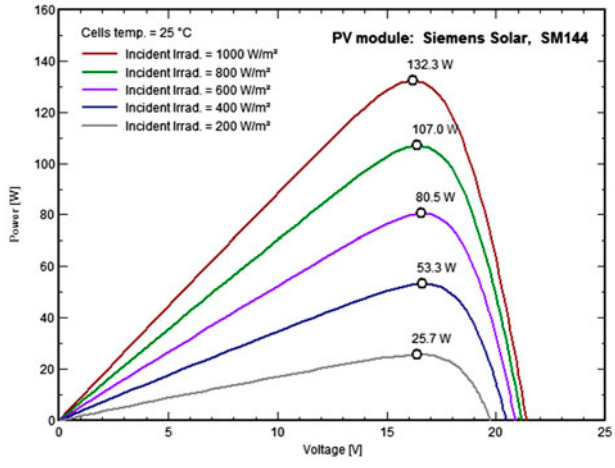

Fig. 17. The effect of solar irradiance on the PV power output of a typical module [12].

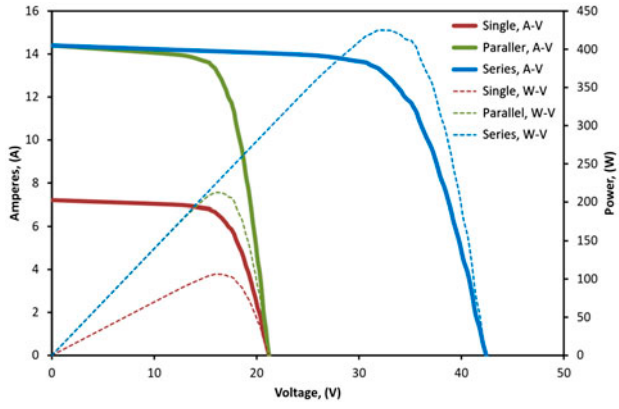

Fig. 19. The effect of joining solar cell in parallel and in series on voltage and current.

The RO system is characterized by:

The specific consumed energy by the RO system is increased with an increase in the feed water salinity. The RO energy consumptions are far less than distillation processes.

It has extensive feed water pretreatment. This pretreatment is a critical part of the system to eliminate or at least to minimize the effect of the fouling which affects greatly the performance and reliability of the RO process. Thus, pretreatment needs serious consideration.

The RO systems have several advantages. It is modular, i.e. it has the flexibility for capacity expansion); and take short construction period. It operates at ambient temperature. The pumps of the RO are usually operated by alternating current (AC), and this necessitates the use of inverter. Batteries also may be required to sustain the RO operation, when solar energy is not sufficient (or smooth its operation when PV output fluctuates). Therefore, the PV system includes PV arrays, batteries, a controller, inverter(s), and several types of load.

Mohsen and Jaber [13] developed a model to determine the specific power delivered for predicted given value range of the global insolation by certain modules, as shown in Fig. 20. The current is expressed in linear relation with global insolation (G) as:

$I = a_1 + a_2G$, and the voltage as $V = K_B \times T/q$, where a_1 and a_2 are model parameters, T is the cell temperature, G is the global irradiance, K_B is the Boltzman's constant and q the electron charge. They used the monthly global solar radiation expressed in terms of the daily average irradiation for four locations in Jordan. The model also expressed the relationship between energy consumption and water salinity for RO system dealing with brackish water as shown in Fig. 20. With brackish water of 2,000 and 5,000 mg/L TDS, the amount of energy required is 1.1 and 1.6 kW h/m^3, respectively, see Fig. 21.

The PV-RO can be stand alone or augmented with other energy source such as wind turbine, Diesel engine, or grid power supply, but most PV-RO applications are stand alone. In the RO system, the use of brine energy recovery system lowers its specific consumed energy, but this is usually limited to high salinity seawater. Several installed PV-RO systems are presented in Table 1.

A schematic diagram for a typical PV powered SWRO pilot plant in a remote area in Gran Canaria (Las Palmas-Spain) system operating in Spain is shown in Fig. 22 [14], and presented here as reference plant. The system has 10 m^3/d product capacities (3 m^3/d for 6 h of operation) with 0.4 recovery ratio (D/F), and 64 bar feed pressure. The high pressure feed pump power consumption is equal to:

$$W_p = \text{Feed } (m^3/s) \times (P\,kPa)/\eta_p$$
$$= [(10/0.4)/(24 \times 3600)] \times (64 \times 100)/(0.75)$$
$$= 2.47 \text{ kW}$$

Calculation is done here for Qatar seawater conditions and not for the reference case, but for the same permeates capacity. The SWRO unit required electric power is about 1.3 of the HP feed water pump, or around 3 kW.

Similarly, electric power, 1 kW, is required to operate the intake pump and pretreatment pumps, as well as 0.75 kW is required to operate the cleaning pump (operating only once the plant is stopped), a total of 4 kW. Therefore, the electric power load ranges from 0.75 to 4 kW. The nominal capacity of the used PV (64 modules × 75 W capacity each) is 5.8 kW$_p$. The ratio of the pumps load (4 kW) to the PV power output (5.8 kW) is the multiplication of inverter (0.9), batteries (0.85), and charger regulator (0.9) efficiencies. The daily PV output is 34.8 kW h for 6 h daily operation.

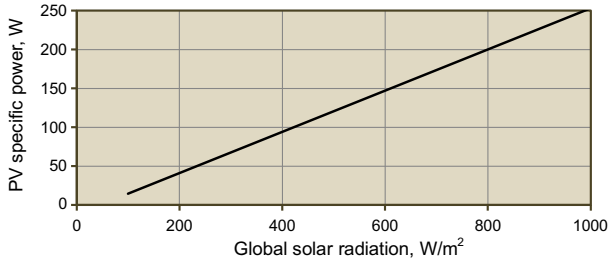

Fig. 20. Specific power vs. global radiation [13].

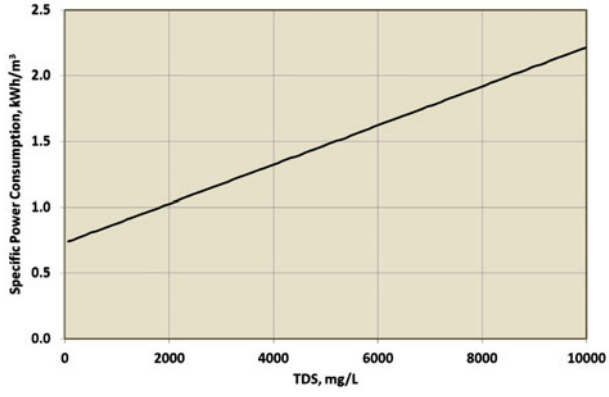

Fig. 21. Energy consumption of RO desalination system as a function of TDS [13].

Table 1
Several PV/RO installed plant [5]

Plant location	Feed water	Plant capacity	Photovoltaic system
Jeddah, SA	42.8 g/l	3.2 m^3/d	8 kW peak
Concepcion del Oro, Mexico	BW	1.5 m^3/d	2.5 kW peak
North of Jawa	BW	12 m^3/d	25.5 kW peak
Red Sea, Egypt	44.0 g/l	50 m^3/d	19.84 kW_p (pump), 0.64 kW_p (control equipment)
Hassi-Khebi Argelie	BW	0.95 m^3/h	2.59 kW_p
Cituis West, Jawa, Indonesia	BW	1.5 m^3/h	25 kW_p
Perth, Australia	BW	0.5–0.1 m^3/h	1.2 kW_p
Wanoo Raodhouse, Australia	BW	–	6 kW_p
Vancouver, Canada	SW	0.5–1 m^3/d	4.8 kW_p
Doha, Qatar	SW	5.7 m^3/d	11.2 kW_p
Thar desert, India	BW	1 m^3/d	0.45 kW_p
North west of Sicily, Italy	SW	–	9.8 kW_p + 30 kW diesel generator
St. Lucie Inlet State Park, FL, US	SW	2´ 0.3 m^3/d	2.7 kW_p + diesel generator
Lipari Island, Italy	SW	2 m^3/h	63 kW_p
Lampedusa Island, Italy	SW	3 + 2 m^3/h	100 kW_p
University of Almeria, Spain	BW	2.5 m^3/h	23.5 kW_p

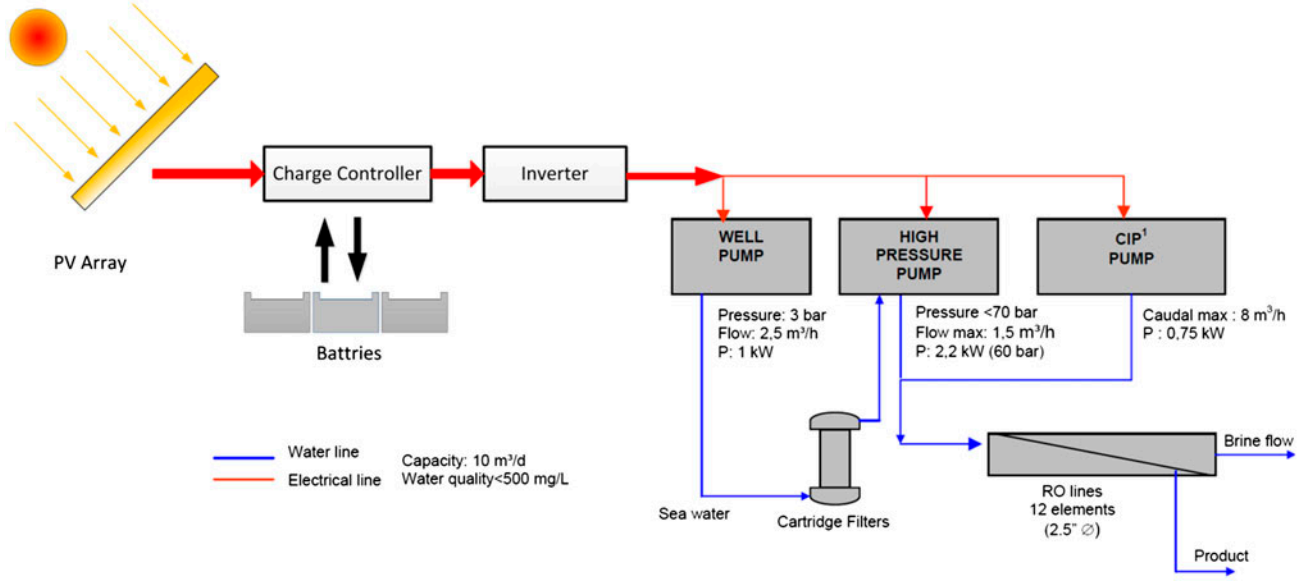

Fig. 22. Diagram of the PV-RO system [18].

For an average daily irradiation of 5.33 kW h/m^2, as example in Doha, Qatar, and 13% PV efficiency, the required area is 34.8/(0.13 × 5.33) = 50.23 m^2.

Some details of the reference case are presented here. The unit produces about 3 m^3/d, on 6 h average operating hours per day. It was built to show the technical and economic viability of the system, and it can be efficiently extrapolated to other productions or qualities. The PV-RO system has a fully automatic control system which manages the power generated and uses it in running the SWRO system on a daily basis, with average of 8 operating hours per day in summer and 6 h in winter (7 h annual average).

The autonomous (PV-SWRO) system, not connected to the grid and using electric energy storage batteries, has 400 L/h production capacity, and 60 bar seawater feed pressure to the membranes.

Batteries are used to solve the PV system principal problem that is the sun does not shine with equal intensity. Daily and annual fluctuations in solar insolation

necessitate storing excess energy for later use. Lead-based batteries are the most commonly employed for this purpose of remote PV system and are the most cost-effective solution for energy storage for small-to-medium-sized autonomous power systems. A battery stores electrical energy in the form of chemical energy. For a PV-battery system to function effectively, the electrochemical processes must work in both directions, i.e. the system must be rechargeable. The batteries have three main functions in a stand-alone PV system: (a) autonomy by meeting the load requirements at all times, including at night, during overcast periods, or during the winter when PV input is low or absent, (b) surge-current capability—by supplying, when necessary, currents higher than the PV array can be delivered, especially to start motors or other inductive equipment, and (c) voltage control to prevent large voltage fluctuations that may damage the load.

The site is at less than 100 m from sea has 2.044 kW h/m mean annual solar radiation, 7.8 m/s mean annual wind speed, 23.5˚C mean annual temperature, and 65–70% mean relative humidity. The SWRO is designed capacity of 10 m/d (24 h), permeate mean conductivity value of less than 1,000 μS/cm and 5.5 kW h/m specific consumed energy and has two parallel lines of 6 spiral-wound membranes each (2.5´´ × 40´´). The pre-treatment includes cartridge filter 25 μm, and cartridge filter 5 μm. The feed water high-pressure pump has feed flow of 900 L/h, 1,000 psi maximum pressure, and is driven by 2.2 kW motor, and high pressure switch 67 bar cut-out pressure. The RO membranes are enclosed in 12 tubes (SW-2540) of 2 m long.

The PV-generating electric power is 4.8 kW_p. The PV field consisting of sixty-four 75 W_p A-75 modules, power accumulation consists of twenty-four 385 ampere-hours (Ah) 2 V vessels, a 75 A regulator, a 4.5 kW inverter and a protection panel with which we separate and protect the panel lines, also including the battery output protection fuses.

The PV field is connected to provide its power to a bank of accumulators, Fig. 23 This process is controlled by a regulator, a device in charge of managing the charge process, preventing the batteries becoming over or undercharged with a view to lengthening their lives as much as possible. Each time the regulator cuts off the charge process, the power provided by the PV generator is lost. This factor is used to design the plant's control program that can practically eliminate these charge cut-out periods, thus making the best possible use of the solar energy available. The accumulators keep the input voltage to the inverter stable and, make it possible to make use of the surplus radiation in the middle of the day, when more power is supplied by the PV system than is consumed by the plant. This surplus is later used to operate the system in the early and late hours of the day, when the process is inverted. This means that the charge regulator never cuts out the charge process, and there is 100% use of the solar energy available. The direct rated voltage of the photovoltaic system, which is 48 V, is transformed by the inverter into 220 V (AC) to adapt it to the plant's operating voltage.

The power storage capacity of the bank of batteries, 19 kW h, is fully optimized, making the installation technically and economically viable. One totally original aspect is measuring the variation in battery capacity in real time by means of a battery monitor with RS232 output, making full use of the solar radiation available and the generation of a large amount of useful information with a view to analyzing battery variations over time. The nighttime use of the battery capacity is not recommended, since this wastes part of the power stored.

The system has a cleaning system that operates when it is shut down on a daily basis to prevent the brine from being in contact with the membranes all night by flushing process. A centrifugal cleaning pump, pumps around 300 L of product water (from the cleaning tanks) at a pressure of about 3–4 bar for flushing process.

To estimate the cost of the PV system, \$6/W_p is assumed for the PV system, or (4.8 × 6,000=) \$28,880, and the cost of the SWRO is \$2,000/(m^3/d) for the small size system. This gives the 10 m^3/d SWRO cost as \$20,000. For 6 h of operation and 3 m^3/d product output, the total cost for one m^3/d is \$16.267/m^3.

The PV-SWRO system has confirmed technical viability. However, its economic viability is doubtful when compared with conventional centralized desalting processes. Its use is justified only in remote areas with no grid connections. A list of some other seawater PV-RO driven plants is given in Table 2. This Table shows that some RO pumps are driven by DC motors, some PV-RO are not using storage batteries, and the high cost of water production [15].

5. Direct and indirect steam operating desalting system

5.1. Energy supply to desalination systems

The desalting plants can be stand-alone driven by a steam boiler, Fig. 24, or by solar collectors, Figs. 4 and 5. When a desalting plant is combined with power plant (PP), it is called CPDP, Fig. 25. Typical CPDP operated with solar collectors replacing the conventional boiler is shown in Fig. 26. Stand-alone DP is

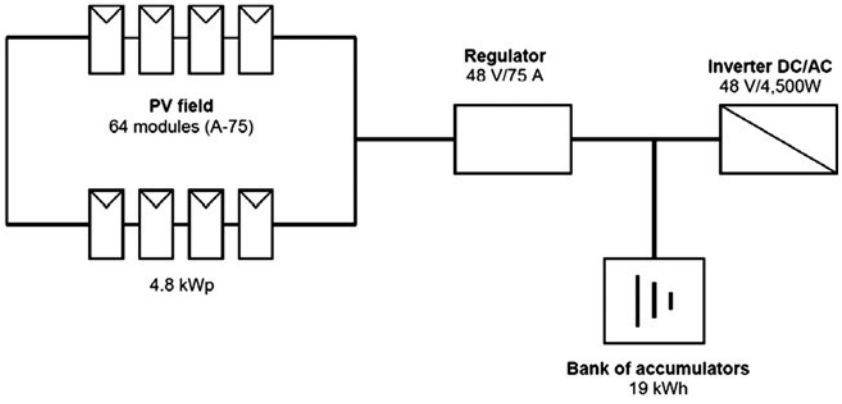

Fig. 23. Diagram of the 4.8 kW_p photovoltaic system [14].

Table 2
Examples of PV driven RO systems [15]

Location and country	Year	Feed TDS (mg/L)	PV Capacity (kW_p)	Battery storage	Pump drive	Production (m^3/d)	Cost ($US/$m^3$)
Abu Dhabi, UAE	2008	45,000	11.25	No	AC	20	7.3
Chania, Crete, GRC	2004	40,000	31.2	Yes	AC	12	8.3
Doha, Qatar	1984	35,000	11.2	No	AC	5.7	3
Jeddah, SA	1981	42,800	8.0	Yes	DC	3.22	6.6
Massawa, UAE	2002	40,000	2.4	No	AC	3.9	10.6
University of Bahrain	1994	35,000	0.11	Yes	DC	0.2	2.8
Pozo, Izquierdo, Spain	2000	35,500	4.8	Yes	AC	1.24	9.6

Notes: It is clear from Table 2 that the specific cost in $US/$m^3$ is very high (6.6–10.6$/$m^3$) for high salinity water seawater. The low numbers given for as $3/$m^3$ for Qatar plant and $2.8 for University of Bahrain plant seem unrealistic.

rarely used in large capacity plant with conventional boiler or solar collectors as it represents an inefficient use of thermal energy.

A typical MSF desalting unit operating in Kuwait, for example, has 24 stages (21 recovery and 3 rejection stages), gain ratio (GR) = 8, (kg distillate product/kg of supplied steam) when operated at TBT = 90.5˚C, and a GR of about 8.6 at TBT = 110˚C. This unit consumes specific thermal energy (Q/D) about 270 MJ/m^3 of DW, [16].

When directly operated with steam generated from boiler of 90% efficiency, the specific consumed fuel energy (Q_f/D) is 300 MJ/m^3. Typical 4 kW h/m^3 pumping (electric) energy is also used to run the MSF unit streams. The specific fuel required to produce this 4 kW h/m^3 (14.4 MJ/m^3) in a power plant having 0.36 efficiency is 40 MJ/m^3). So, the specific fuel required to provide both thermal energy and pumping power is 340 MJ/m^3. For a barrel of oil (having 6 GJ energy)

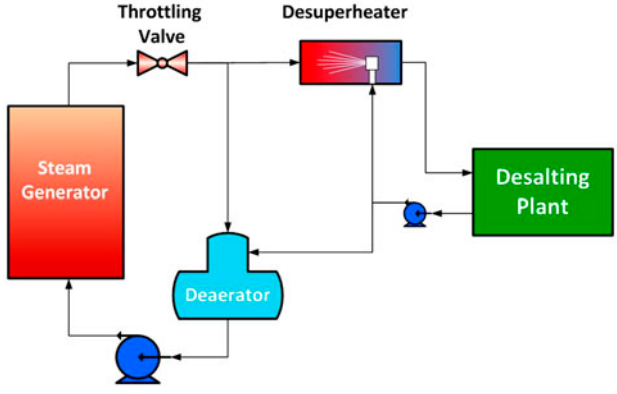

Fig. 24. Steam generated by fossil fuel to directly operate desalting plant.

and costing $60, the fuel energy used to produce one m^3 is (340/6,000) × 100 ~ $3.36/$m^3$. This is very high to produce one m^3. Even if NG having 60% of oil

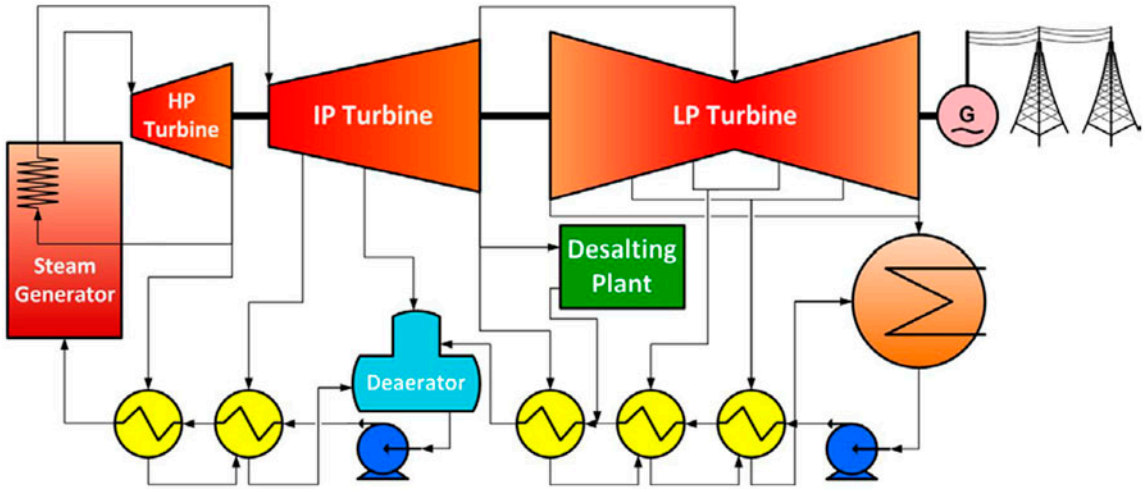

Fig. 25. CPDP using fossil fuel with steam extracted to the DP from cross line between the intermediate and low-pressure turbines.

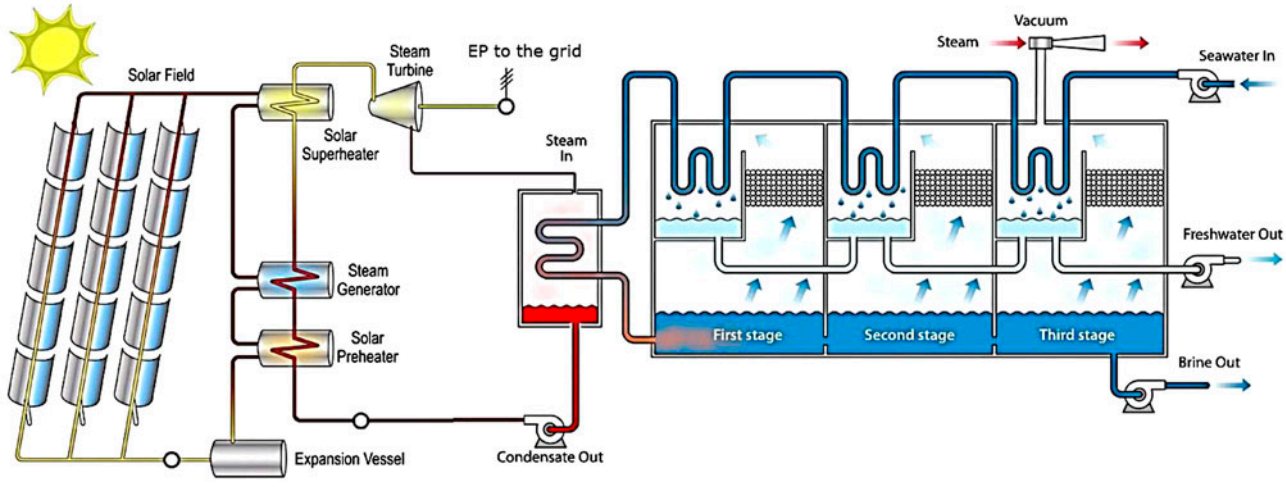

Fig. 26. Typical CPDP with MSF distillation system and electric power to the grid.

price is used, the specific fuel cost would be still high at \$2.02/m^3.

In CPDP, steam plant operating by fuel, Fig. 25, or by solar energy, Fig. 26, steam is generated at much higher temperature and pressure than those required by the MSF unit. This steam is supplied to a steam turbine and expands to produce work, i.e. electric power before its extraction (or discharge) to the desalting plant. The cost of producing steam is shared by the produced electric power and DW. In a typical CPDP using steam turbine, if one kg of steam at the condition of steam extracted to the MSF unit is introduced to a low pressure steam turbine, it produce about 490 kJ of work. This work is considered as work loss due to supply of the steam to the DP, rather than its expansion to the condenser condition. For a typical MSF unit having 8.5 gain ratio (GR) defined by desalted water/steam supply, the work loss due supplying thermal energy of 270 kJ/kg of DW is equivalent to work equal 490/8.5 = 57.6 kJ/kg of DW (16.01 kW h/m^3). By adding pumping work (about 4 kW h/m^3) to the 16.01 kW h/m^3, the mechanical equivalent energy to the thermal consumed energy and pumping, the total equivalent work is about 20 kW h/m^3 (72 MJ/m^3). To produce this amount of work in power plant of 0.36 efficiency, it needs about 200 MJ/m^3. This is to be compared with 340 MJ/m^3 for stand-alone (or about 41% reductions in fuel

energy). This applies to CPDP using fossil fuel or solar energy. Again for a barrel of oil (having 6 GJ energy) and costing \$60, the fuel energy used to produce one m^3 in CPDP is $(200/6{,}000)\times 60 = \$2/m^3$. This is still very high to produce one cubic meter. Even if NG having 60% of oil price is used, the specific fuel cost would be still high at $\$1.2/m^3$. This is the main reason for using CPDP as illustrated later. Close results for CPDP) were reported by ESCW, [17]. In conclusion, the steam is usually generated at high availability (i.e. high pressure and temperature). When supplied to CPDP, it expands and produces work before its availability is reduced to that required by the MSF plant, when it is extracted. When the steam from steam generator is directly supplied to the MSF units, it is throttled to the availability and conditions required by the MSF without producing work. In CPDP, the fuel used to produce steam is shared by the work output and desalted water in CPDP, while it is completely charged to desalted water in the other case.

5.2. SPPs using PTC

Several types of solar collectors are used to transfer solar energy to thermal energy to operate the SPPs. These include linear Fresnel solar collectors (LFC), and PTCs that concentrate solar rays on line collectors; and central receivers (towers) and parabolic dishes concentrating solar rays on point collectors. The SPP using solar PTC and steam Rankine heat engine is the well proven and mostly used type. The PTC has troughs-curved mirrors that reflect the incident direct solar radiation onto collector tubes (called a receiver, absorber or collector), Fig. 27. The receiver tube is positioned along the focal line of the trough, contains running fluid that absorb the received heat. The trough is parabolic along one axis and linear in the orthogonal axis. The sunrays are kept perpendicular and focused on the receiver most of the time by tilting the trough to face east to west. Therefore, the trough is practically uses tracking on a single axis. The receiver is usually enclosed in a glass vacuum chamber, with fluid passing through the receiver called heat transfer fluid (HTF). Its temperature is raised to high temperatures (390˚C). The HTF is usually synthetic oil. The hot HTF is used in heat exchangers to generate steam operating Rankine steam power cycle. Full-scale PTC systems consist of many such troughs laid out in parallel over large land area (4–5 times the solar collectors' area) [18].

The history of SPPs using PTCs goes back to the solar electric generation system (SEGS) plant operating in California (CA), USA since 1985, see Table 3. Trough plants generate their peak output during sunny periods when air conditioning loads are at their peak. Integrated SPPs, with NG-operated boilers and/or thermal storage have allowed the plants to provide firm power even during non-solar and cloudy periods. The long time operation experience by the SEGS make this type of SPP a well proven and the most used type. The PTC accounted for about 96% of global concentrated solar power (CSP) capacity at the end of 2010; tower technology accounted for 3%.

Data on some of the SEGS and Nevada solar 1 are given in Table 3, and on some of Spain parabolic trough SPP are given in Table 4, [19]. At the end of 2010, Spain accounted for about 57% of all global CSP capacity. The Andasol 1, Andasol 2, and Andasol 3 plants shown in the table are the first commercial CSP plants to feature thermal energy storage (TES), using two tank of molten salts to store up to 7.5 h of peak-loaded energy, [19]. Two other large projects in USA are the Mojave Solar Park and Beacon solar project.

The data given in Tables 3 and 4 indicate that the specific field collector size per MW is in the range of 6,000 m^2/MW without TES; and 10,000 for 7.5 h of TES. The reported direct normal irradiance (DNI) in Spain is around 2,168 kW h/m^2/y (close to that in Qatar), while 2,700 kW h/m^2/y were reported in CA, US. The HTF inlet and outlet temperature are 293 and 393˚C, respectively, and thus the throttling condition of Rankine power cycle is about 370˚C. The steam pressure at the steam turbine inlet is 100 bar. This necessitates the use of reheat turbine to insure at least 88% dryness fraction at the turbine exit as required by the steam turbines industry. The cycle has an average annual solar to electricity efficiency of 16%.

5.3. Reference SPP

A reference plant, Fig. 27, is chosen here similar to the SEGS VI of 30 MW located in CA using a collector type known as LS-2, and another 30 MW planned for Pakistan using Euro-trough collectors (ET 150), where direct solar radiation is close to that in Qatar, i.e. more than 1,900 kW h/m^2/year (5.2 kW h/m^2/d), [20]. The solar field consists of 56 loops, and each loop has 4 solar collector assembly (SCA) of 148.5 m length, and 5.77 m aperture area of ET 150 collectors. The total aperture collector area is 191,933 m^2, producing 118.2 MW_{th} thermal energy, and electric power of 31.4 MW_e. The main characteristics of ET150 are given in Table 5. This gives solar specific collector area of 6,085 m^2/MW_e, and 1,624 m^2/MW_t. The collectors are aligned on a north–south line, thus tracking the sun as it traverses the sky from east to west. The reflectors are made up of a

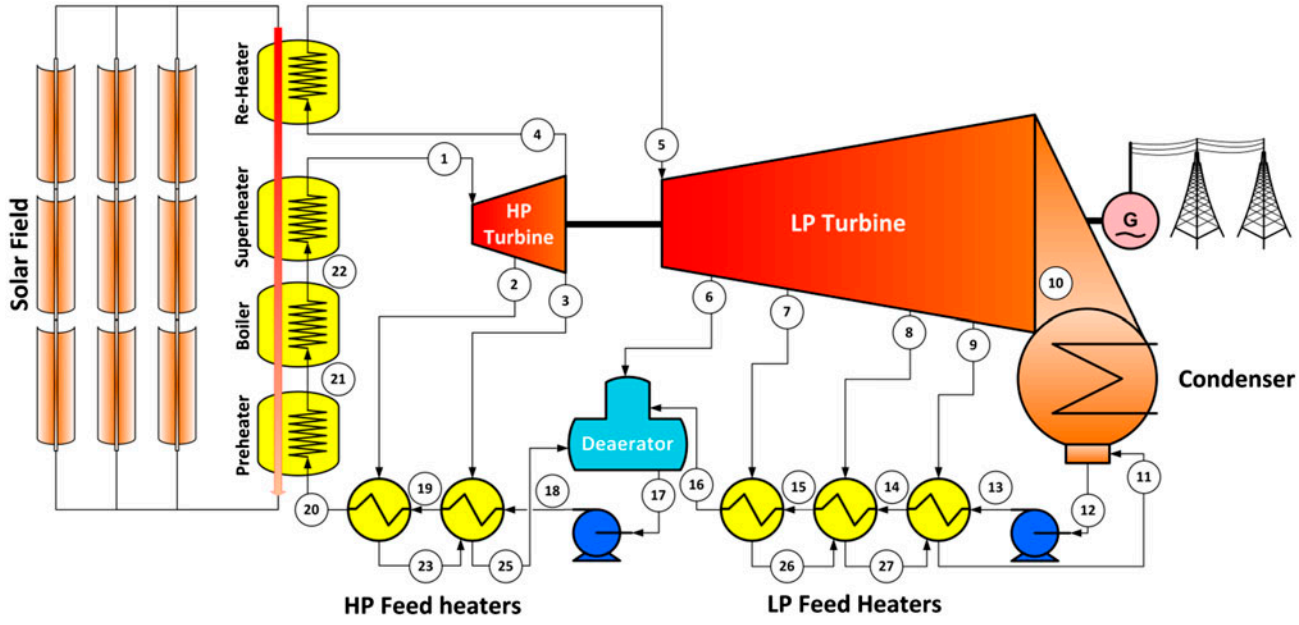

Fig. 27. Schematic diagram of the reference plant steam cycle with points.

Table 3
Basic characteristics of some SEGS parabolic trough SPP at Kramer Junction and Nevada Solar 1 [19]

Plant name	Start-up year	Capacity (MW)	Solar field temp. (°C)	Solar turbine efficiency (%)	Solar field size (m^2)	Power cycle pressure (bar)	Dispatch-ability
SEGS III	1987	30	349	30.6	230,300	40	Gas boiler
SEGS VI	1988	30	390	37.50	188,000	100 (reheat)	Gas boiler
SEGs IX	1991	80	390	37.60	483,960	100 (reheat)	HTF heater
Nevada solar 1	2007	64	390	37.60	357,200	100 (reheat)	None

number of submodules each with a typical length of 12 m. The ET150 has an overall length of 150 meters (m) length and aperture width of 5.77 m, and consists of 12 submodules [21]. There are 56 solar trough collector groups mounted on SCA, Figs. 28a–28c.

The plant, similar to that shown in Fig. 27, has five closed feed water heaters (FWH), and one open FWH (de-aerator). Steam condition to the HP turbine inlet point (1) is 370°C temperature, 100 bar pressure, and 36 kg/s steam flow rate (assumed and to be checked). The Rankine cycle state points are given in Table 6, [19].

The current investment cost for PTC plants without storage ranges between \$4,500/kW and \$7,000/kW. The use of TES increases the capital cost, but allow higher capacity factors. The reported investment cost of 50 MW showed that the solar field and HTF and system cost is \$140.3 M, or \$2.8 M/MW_e plus site and solar field preparation of \$62.4 M, or \$1.248 M/MW_e. Therefore, the total solar field cost for the reference plant is \$121.62 M, (\$1.248/MW_e), or a total of \$202.7 M and \$4.054/MW_e. So, the cost of complete solar collector field with preparation is \$121.62 M, and for the area of 191,933 m^2 the cost of collector/m^2 is \$634/m^2. The power block \$M31.2 or \$1.04/MW_e. So, the total plant capital cost is 152.82 M (\$5.1/MW_e).

5.4. Modified reference SPP to include desalting plant

In order to compare the capital cost when the DP is standing alone or when combined with SPP at several configurations, the reference plant shown in Fig. 27 is modified as shown in Fig. 29. In this modification, the turbine is changed from extraction condensing steam turbine to back pressure steam turbine with all its discharged steam is supplied to MED. Therefore, the condenser and the last part of turbine from point 8 to the end condenser inlet (at

Table 4
Basic characteristics of the parabolic trough SPP in Spain [19]

Name	Capacity (MW)	Storage hours	DNI (kW h/m^2/y)	Solar field area (As/MW)	Plant (1,000 m^2/MW)	ε (kW h)	Temp. solar field in/out	Efficiency
Alvarado-1	50		2,174		27	27	293/393	
Andasol-1	50	7.5	2,136	10,202.4	40	27	293/393	16
Andasol-2	50	7.5	2,136	10,202.4	40	27	293/393	16
La Florida	50	7.5		11,055.0	40	27	298/393	14
Extresol-2	50	7.5	2,168	10,202.4	40	27	293/393	16
Extresol-1	49.9	7.5	2,168	10,222.9	40	27	293/393	16
Ibersol Ciudad Real	50	0	2,061	5,755.2	30		304/391	
La Dehesa	49.9	7.5		11,077.2	40		29/393	14
Majadas	50		2,142			27		
Manchasol-1	49.9		2,208		40		293/393	16
Palma del Rio-2	50	0	2,291		27	27	293/393	

Table 5
Main characteristic parameters of EuroTrough 100 and 150 m [21]

EuroTrough model	ET100	ET150
Focal length (m)	1.71	1.71
Absorber radius (cm)	3.5	3.5
Aperture width (m)	5.77	5.77
Aperture area (m^2)	545	817.5
Collector length (m)	99.5	148.5
Number of modules per drive	8	12
Number of glass facets	224	336
Number of absorber tubes (4.1 m)	24	36
Mirror reflectivity (%)	94	94
Weight of steel structure and pylons, per m^2 aperture area, kg	19.0	18.5

point 10), and two feed heaters are omitted. The omitted part of the turbine is most expensive and least efficient part of the turbine. So, the power block is expected to decrease to 60% of its original cost. The desalination system is chosen to be MED with TBT equal to 70°C, and the gain ratio $D/S = 8$. The BPST discharge condition is expected to be at point 8 where the steam is at 0.96 bar, and 99°C saturation temperature to overcome the problem of decreasing pressure at part load. At full load, the steam at point 8 should be throttled to the pressure required by the desalting plant. Accordingly for the same steam flow rate of the turbine inlet (36 kg/s), the work loss between point 8, and end condenser was calculated as $W_{dc} = W_{9-10} + W_{8-9} = 7{,}379.4$ kW. The discharged flow rate is 27.06 kg/s, and thus the MED plant capacity is $D = 27.06 \times 8 = 216.45$ kg/s. Therefore, the specific equivalent work (W_{dn}/D) to thermal energy supplied to the desalination plant is: $W_{dn}/D = 30.7$ kJ/kg (8.52 kW h/m^3), and the equivalent work for the LT-MED including pumping energy (2 kW h/m^3) is 10.52 kW h/m^3. The steam supplied to the desalination plant is discharged from the steam turbine at 2,650 kJ/kg enthalpy, and leaves as saturated liquid at 70°C (293.07 kJ/kg enthalpy). So the heat gained by the DP is $Q_d = 27.06(2{,}650–293.07) = 63{,}778.5$ kW, and the specific heat in kJ/kg of desalted water (D) is $Q_d/D = 294.6$ kJ/kg. The back pressure steam turbine work output would be $W_n = 23{,}358$ kW. Now, the reference SPP and its modified version are used to evaluate several versions of using solar energy for desalination.

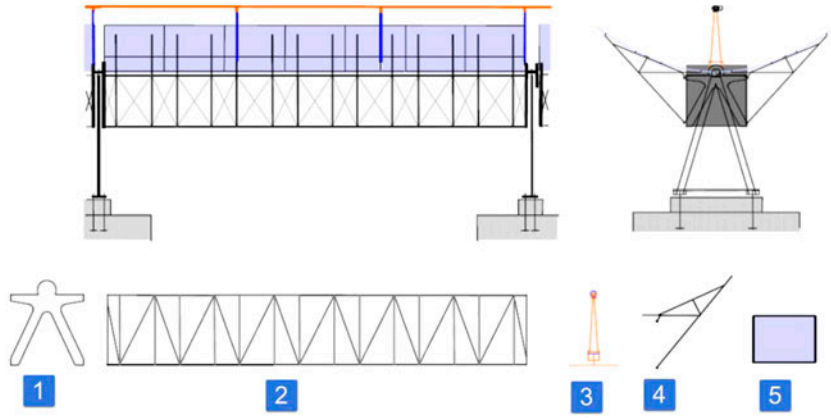

Fig. 28c. Euro-trough module structural elements: (1) front and rear endplates for mounting to the pylons, (2) space frame structure, (3) receiver supports, (4) cantilever arm, (5) mirror facet [19].

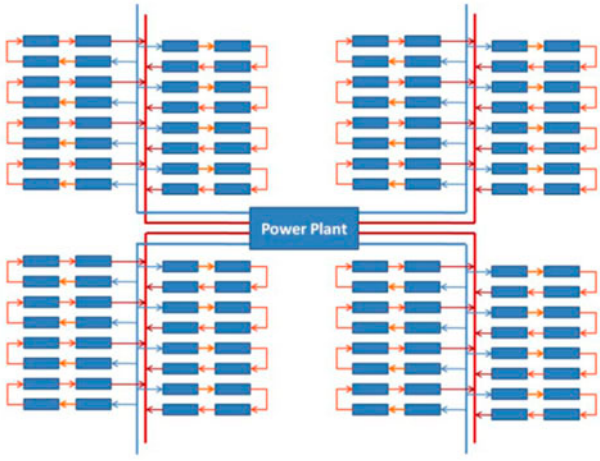

Fig. 28a. Solar field layout [20].

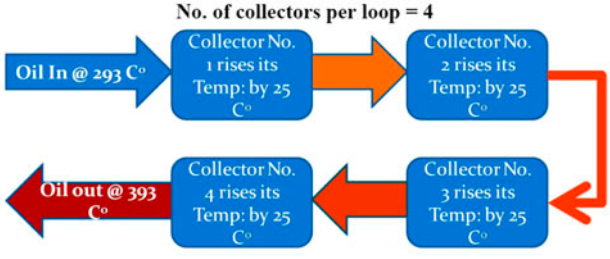

Fig. 28b. A collector loop raising the temperature of HTF by 100°C, [20].

Version 1: directly operated desalting system

(1) Direct solar operated MSF units: in this case, only the PTC used in the reference SPP, and produces 118.2 MW thermal energy operates an MSF units of GR = 8.5 consuming 270 MJ/m^3 thermal energy and 4 kW h/m^3 pumping energy (equivalent to 40 MJ/m^3 thermal energy), the desalting plant output would be (32,943 m^3/d or 7.25 MIGD). In this case, the PTC costing \$121.62 M is used to produce 7.25 MIGD, or \$16.78 M/MIGD. The capital cost MSF is in the range of \$1,800/m^3, or the desalination plant cost would be \$M 59.3, and the total cost of the PTC and desalting plant is \$M180.947, or \$5,492/(m^3/d).

(2) Direct solar operated MED units: in this case, only the PTC used in the reference SPP, and produces 118.2 MW thermal energy that operates an MED units of GR = 10, consuming 230 MJ/m^3 thermal energy and 2 kW h/m^3 pumping energy (equivalent to 20 MJ/m^3 thermal energy), the desalination plant output would be (40,845 m^3/d or 8.96 MIGD). In this case, the cost of the PTC costing \$121.62 M is used to produce 8.985 MIGD, or \$13.54 M/MIGD. The capital cost ME-TVC is in the range of \$1,500/m^3, or the desalination plant cost would be \$M 61.27, and the total cost of the PTC and desalting plant is \$M182.888, or \$4,478/(m^3/d).

Version 2: SPP operating desalting system

(1) SPP operating SWRO: in this case, the EP output of 30 MW_e of the reference SPP is used to operate the SWRO desalting plant consuming 5 kW h/m^3 (18 MJ/m^3 mechanical energy, the DP output would be 144,000 m^3/d or 31.68 MIGD). In this case, the cost of the SPP is \$M 152.82 M, the cost SWRO plant (in \$M) is (144,000 × \$1,100/(m^3/d)/1,000,000) = \$M

Table 6
The state points of the reference plant steam cycle

State point	Mass flow rate (kg/s)	Pressure (bar)	Temp. (°C)	Enthalpy (kJ/kg)
1	36	100	370	3,005
2	2.7	33.61	238	2,807
3	2.575	18.58	207	2,710
4	30.725	18.58	207	2,710
5	30.715	17.1	370	3,190
6	2.0245	7.98	278	3,016
7	1.634	2.73	168	2,798
8	1.498	0.96	99	2,650
9	1.021	0.29	70	2,500
10	24.5375	0.1	45.81	2,350
11	30.725	–	45	–
12	30.725	–	45	–
13	30.725	14.76	45	188
14	30.725	10	65	271.7
15	30.725	8.7	95	398.9
16	30.725	7.94	127	532.7
17	36	7.94	–	
18	36	125	170	722.5
19	36	112	–	873.2
20	36	103	–	1,014.8
21	36	100	311	1,407.8
22	36	100	311	2,725.5

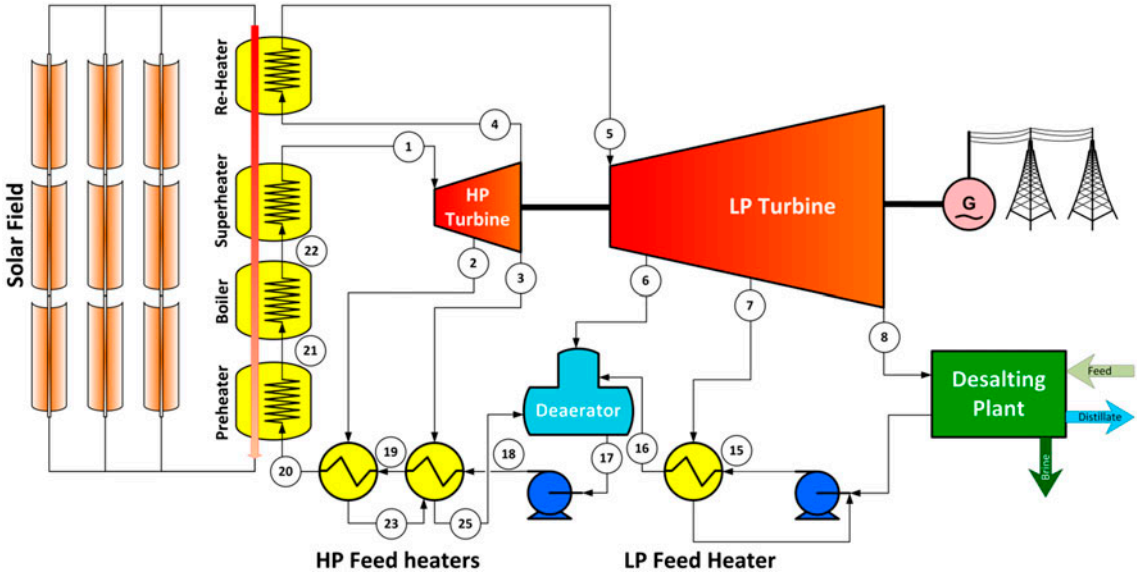

Fig. 29. Schematic diagram of modified reference SPP with BPST discharging its steam to MED plant.

158.4, and the investment cost is \$M311.22 or \$2,161/(m^3/d).

(2) SPP operating MVC: In this case, the EP output of 30 MW_e of the reference SPP is used to operate the MVC desalting plant consuming 10 kW h/m^3 (36 MJ/m^3 mechanical energy), the DP output would be (72,000 m^3/d or 15.838 MIGD). In this case, the cost of the SPP is \$152.82 M, and the cost is desalting plant is (72,000 × \$1,100/(m^3/d)/1,000,000) = \$M 79.2

Table 7
Comparison of the capital cost of energy systems when PTC is used to produce thermal energy that directly operate DP or through SPP

Cases	DW (m^3/d)	Equipment capital cost ($M)	Specific capital cost ($/($m^3$/d))
PV-SWRO	3	48,880	16,293
1a (PTC + MSF)	32,943	181,000	5,492
1b (PTC + MED)	40,845	183,000	4,478
2a (SPP + SWRO)	144,000	311,000	2,161
2b (SPP + MVC)	72,000	311,000	3,223
2c (SPP + SWRO + MED)	130,834	296,000	2,266

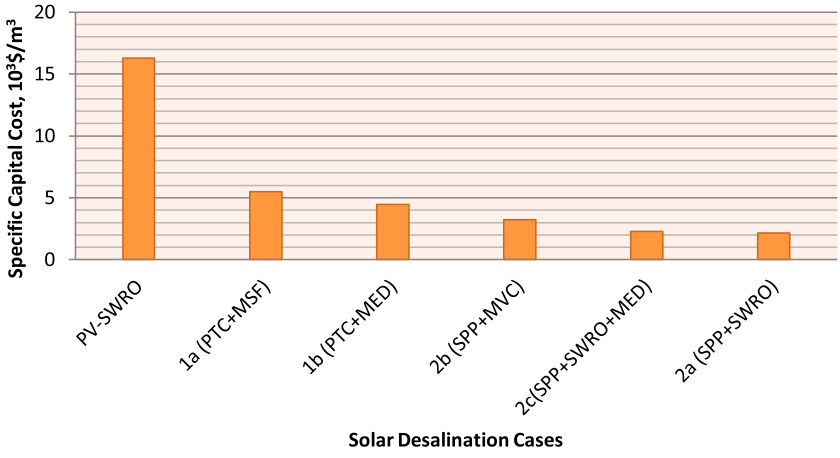

Fig. 30. Capital cost of energy system.

and the investment cost is $M232.02 or $3,223/($m^3$/d).

(3) Back pressure SPP operating MED: in this case, the modified SPP producing EP output of 23.358 MW_e, and supplying extracted steam of 27.06 kg/s to an MED plant. The EP output operates an SWRO plant consuming 5 kW h/m^3 (18 MJ/m^3 mechanical energy) and produces 112,118 m^3/d or 24.663 MIGD. The 27.06 kg/s extracted steam to the MED plant of GR = 8 produces 216.48 kg/s (4.11 MIGD or 18,704 m^3/d). Now the total DW output is 28.78 MIGD (130,834 m^3/d). The capital cost for this case is the $121.62 M for the PTC, and 75% of the power block cost $18.72 M, a total cost of $145.02 M. The capital cost of the desalination plants is: 112,118 × $1,100/($m^3$/d)/$10^6$ = $M 123.33 for the SWRO plant and 18,704 × $1,100/($m^3$/d)/$10^6$ = $M 28.056 for the MED plant. So, the total investment cost is 145.02 + 123.33 + 28.056 = $M 296.406, or $2,266/($m^3$/d).

A brief comparison between the above cases of transforming the solar energy to thermal heat to directly operate DPs or through SPP is presented in Table 7 and Fig. 30. It shows that operating the thermal desalting plants directly by PTC is very expensive, and cost 2–3 times the cost of using SPP to operate the most economic desalting plant of SWRO system.

Comparison of the high specific cost of small capacity PV-SWRO with that of large capacity solar thermal desalting systems is not realistic, as the first is serving specialized purpose in remote area.

6. Conclusion

The use of solar energy to produce DW is an attractive choice for the GCC, where DW demands are continuously increased. The sustainable use of solar energy would decrease burning of finite fossil fuel and its GHG emission, where Qatar and UAE have the highest per capita emission in the world. Solar

desalination by photovoltaic (direct conversion from solar energy to EP) to drive RO or MVC; or solar thermal energy to drive distillation system directly or indirectly through SPP was reviewed. The use of PV to operate RO is very expensive due to the high expenses of both PV and batteries and should be limited only to remote areas with no water resources, and/or water transportation is very expensive. As shown from the calculations, a 10 m^3/d SWRO system produces only 3 m^3/d; since the system is operated only during sun shining time. The specific capital cost of the PV-RO system is \$16,293/(m^3/d). The conversion of solar energy into thermal energy supplied directly to thermal operated DPs is much cheaper than the PV-RO system. The specific capital cost of the CSP-thermally operated desalination systems ranges between 4,500 and 5,500\$/(m^3/d). However, this is still much higher than the use of solar energy to produce heat and operate SPP, where the specific capital cost of the system is in the range of \$2,200–\$3,200/(m^3/d). Using solar energy to operate SPP to drive RO, and its extracted steam to run MSF or ME has the lowest specific capital cost of the modeled systems.

References

[1] T. El Sayed, J. Ayoub, Achieving a sustainable water sector in the GCC: Managing supply and demand, building, Online Report published May 8, 2014. Available from: <http://www.strategyand.pwc.com/media/file/Strategyand_Achieving-a-sustainable-water-sector-in-the-GCC.pdf>.

[2] A. Al-Alshaikh, IDA R&D Committee: An Overview, in: Desalination Research Centers, Achievement & Future Trends Workshop on 17–19 March 2013 Hilton Hotel Jeddah Saudi Arabia. Available from: <http://idadesal.org/wp-content/uploads/2013/05/IDA_RD-Committee-Meeting-Combined-Overview-Presentations-Day-1.pdf>.

[3] M.A. Darwish, MSF Engineering, in Thermal Desalination Processes, from Encyclopedia of Desalination and Water Resources, EOLSS Publishers, Paris. Available from: <http://www.desware.net> (Retrieved November 24, 2014).

[4] M.A. Darwish, Fundamentals of Multiple Effect Evaporation, in Thermal Desalination Processes, from Encyclopedia of Desalination and Water Resources, EOLSS Publishers, Paris. Available from: <http://www.desware.net> (Retrieved November 27, 2014).

[5] A.M. El-Nashar, Desalination With Renewable Energy—A Review, in Renewable Energy, in Encyclopedia of Life Support Systems (EOLSS), Developed under the Auspices of the UNESCO, EOLSS Publishers, Oxford, UK. Available from: <http://www.eolss.net> (Retrieved November 21, 2014).

[6] D. Feldman, G. Barbose, R. Margolis, N. Darghouth, T. James, S. Weaver, A. Goodrich, R. Wiser, Photovoltaic System Pricing Trends: Historical, Recent, and Near-Term Projections, Online Report by SunShot US Department of Energy, 2013 Edition. Available from: <http://emp.lbl.gov/sites/all/files/presentation.pdf>.

[7] Solarbuzz, Module Pricing. Available at: <http://solarbuzz.com/facts-and-figures/retail-price-environment/module-prices> (accessed: January 2012).

[8] G. Schumm, Solar Photovoltaic Energy Conversion, in Renewable Energy Systems and Desalination, from Encyclopedia of Desalination and Water Resources, EOLSS, Publishers, Paris. Available from: <http://www.desware.net> (Retrieved November 25, 2014).

[9] P. Govinda Rao, M. Mohd Saeed Al-alshaikh Al-Kuwari, Assessment of solar and wind energy potential in Qatar, Second joint Qatar-Japan Environment Symposium, 05–06 February 2013, Doha-Qatar. Available from: <https://www.jccp.or.jp/international/conference/docs/14assessment-of-solar-and-wind-energy-potential-in.pdf>.

[10] Average Weather for Doha, Qatar. Available from: <https://weatherspark.com/averages/32878/Doha-Ad-Dawhah-Qatar> (accessed July 30, 2015).

[11] A. Murray Thomson, Reverse-Osmosis Desalination of Seawater Powered by Photovoltaics Without Batteries, Ph.D. Thesis, Loughborough University, UK, 2003.

[12] R. Waked Assad Al-Qutub, Treatment of Surface Water by Autonomous Solar-Powered Membrane Cells, M.Sc. Thesis, An-Najah National University, Palestine, 2010.

[13] M.S. Mohsen, J.O. Jaber, A photovoltaic-powered system for water desalination, Desalination 138 (2001) 129–136.

[14] T. Espino, B. Peñate, D. Henríquez, J. Betancort, G. Piernavieja, Seawater desalination plant by reverse osmosis powered with photovoltaic solar energy: A supply option for remote areas. Available from: <http://www.renovae.org/index.php?option=com_docman&task=doc_download&gid=15&Itemid=44> (accessed November 24, 2014).

[15] A. Ghermandi, R. Messalem, Solar-driven desalination with reverse osmosis: the state of the art, Desalin. Water Treat. 7 (2009) 285–296.

[16] M.A. Darwish, Thermal desalination in GCC and possible development, Desalin. Water Treat. 52 (2014) 27–47.

[17] Role of Desalination in Addressing Water Scarcity: Economic and Social Commission for Western Asia (ESCWA), Water development report 3, E/ESCWA/SDPD/2009/4, United Nations. Available from: <http://www.bookish.com/books/escwa-water-development-report-3-united-nations-9789211283297> (accessed November 28, 2014).

[18] D.W. Kearney, Parabolic Trough Collector Overview. Available from: <http://www.nrel.gov/csp/troughnet/pdfs/2007/kearney_collector_technology.pdf> (accessed November 28, 2014).

[19] M.A. Darwish, A. Darwish, Solar cogeneration power-desalting plant with assisted fuel, Desalin. Water Treat. 52 (2014) 9–26.

[20] S. Saleem, A. ul Asar, Analysis & Design of Parabolic Trough Solar Thermal Power Plant for Typical Sites of Pakistan, IOSR J. Electr. Electron. Eng., e-ISSN: 2278-1676, p-ISSN: 2320-3331, 9(3) (2014) 116–122.
[21] M. Geyer, E. Lüpfert, R. Osuna, A. Esteban, W. Schiel, A. Schweitzer, E. Zarza, P. Nava, J. Langenkamp, E. Mandelberg, EUROTROUGH—Parabolic Trough Collector Developed for Cost Efficient Solar Power Generation, 11th SolarPACES International Symposium on Concentrated Solar Power and Chemical Energy Technologies, September 4–6, Zurich, Switzerland, 2002.